WAVEFORM OPTIMIZATION FOR COMPRESSIVE SENSING RADAR SYSTEMS

Lyubomir Zegov[†], *Radmila Pribić*[*], *Geert Leus*[†]

[†]*l.t.zegov@student.tudelft.nl*, [†] Delft University of Technology, Delft, The Netherlands
[*]Sensors Advanced Developments, Thales Nederland, Delft, The Netherlands

ABSTRACT

Compressive sensing (CS) provides a new paradigm in data acquisition and signal processing for radar. In this work, we investigate the performance of several deterministic waveforms for the basic problem of range-only estimation in CS-radar system. We investigate the effects of a digital RF system - from signal generation at the transmitter, to sparse signal recovery at the receiver, on the incoherence of the received signal. We demonstrate the capabilities of CS-radar versus the conventional pulse compression radar.

***Index Terms*—** radar, compressive sensing, waveforms, optimization

1. INTRODUCTION

Compressive sensing (CS) offers a new perspective for signal acquisition and recovery, based on the sparsity and incoherence of the unknown signal. Under those conditions, the unknown signal can be recovered even from a possibly underdetermined linear system. In radar, the incoherence is tightly related to the well known autocorrelation function (ACF) of the transmitted pulse. Most works on optimal waveforms in CS-radar do not consider the effects of the radio frequency (RF) system on the received signal [1, 2], or assume random signal acquisition [3]. Due to the specific considerations that are made for a radar transceiver, e.g., operation of the power amplifier in saturation, cost and complexity, the intention is to utilize constant amplitude deterministic waveforms.

In this work, we investigate several candidate deterministic waveforms for implementation in a CS-radar system. The optimality of those waveforms is defined based on the width of the main lobe and the level of the off-peak correlations in the ACF, and concerning the RF System - the required double-sided transmission bandwidth, as well as the ease of generation, transmission and reception.

In Section 2, we introduce the data model for a CS-based radar for range-only estimation, and establish the notation. Then, in Section 3 we present the model of the digital RF system, while Section 4 and Section 5, respectively, show our results on the optimization of the waveforms and the recovery results. Finally, we draw some conclusions in Section 6.

2. CS RADAR DATA MODEL

We are interested in the detection of stationary targets in the unambiguous range interval $[\rho_1, \rho_2]$. Discretization of $[\rho_1, \rho_2]$ into QN bins (range gates), each with size $\Delta\tau = 1/(Qf_s)$, defines the estimation grid $[\tau_1, \dots, \tau_{QN}]$, where each cell τ_k, is related to a target with magnitude $x_k, k = 1, 2, \dots, NQ$. The sampling frequency $f_s = 1$ is the reference sampling frequency, normalized to the double-sided bandwidth $B_s = 1$ of a linear frequency modulated (LFM) pulse, and we refer to the grid, with cells of size $\Delta\tau = 1/f_s$, as the reference estimation grid.

If the transmitted analog pulse $s_a(t)$ has length L/f_s, then the received signal $r(t)$ has length P/f_s, where $P = N + L - 1$. Sampling $r(t)$ at the reference frequency f_s, we obtain the vector $\mathbf{r} \in \mathbb{C}^{P\times 1}$, which contains the radar echoes $\mathbf{y}$ corrupted by Gaussian noise $\mathbf{e} \sim \mathcal{CN}(\mathbf{0}, \sigma^2\mathbf{I})$, with $\mathbf{I}$ an identity matrix of size $P \times P$. Then the radar echo can be written as

$$\mathbf{y} = \mathbf{S}\mathbf{x}, \tag{1}$$

where $\mathbf{S}$ is the model matrix and $\mathbf{x} \in \mathbb{C}^{NQ\times 1}$ contains the unknown target magnitudes x_k . The (n, k)-th entry of $\mathbf{S}$ is related to the transmitted analog pulse $s_a(t)$ as:

$$\mathbf{S}_{n,k} = s_a(n/f_s - k/(Qf_s)). \tag{2}$$

In case $Q > 1$, we obtain a finer resolution $\Delta\tau = 1/(Qf_s)$, while sampling at the reference rate f_s at the receiver , which leads to an underdetermined system in (1).

Furthermore, CS offers a way to reduce the number of measurements P, with a factor C, while keeping the reference resolution $\Delta\tau = 1/f_s$, by application of a compression matrix $\mathbf{\Phi} \in \mathbb{C}^{\lfloor P/C\rfloor\times P}$, where $\lfloor\cdot\rfloor$ denotes the floor function. Also in this case, we get an underdetermined system $\mathbf{r} = \mathbf{\Phi}\mathbf{S}\mathbf{x} + \mathbf{\Phi}\mathbf{e}$. The condition on $\mathbf{\Phi}$ is to be incoherent with $\mathbf{S}$, while the specific choice of $\mathbf{\Phi}$ is to the user [4].

In the above mentioned underdetermined problems, $\mathbf{x}$ can be recovered if $\mathbf{S}$ or accordingly $\mathbf{\Phi}\mathbf{S}$ satisfy the restricted isometry property (RIP) [5], which guaranties the incoherence. A simpler measure of the incoherence of a matrix is the mutual coherence $\mu(\mathbf{S})$, given by the largest inner product $\mu(\mathbf{S}) = \max_{i\neq k} |\langle\mathbf{s}_i, \mathbf{s}_k\rangle|$ between the normalized columns $\mathbf{s}_i$ of $\mathbf{S}$, e.g., $||\mathbf{s}_k||_2 = 1,\ k = 1, 2, \dots, NQ$, where $||\cdot||_2$

marks the ℓ_2 norm of a vector, which we will use in Section 4 to judge the quality of the investigated waveforms.

3. RF SYSTEM

We model the radar system as a general digital RF system as shown in Fig. 1. A typical realization of such a system will require a fast DAC, ADC and DDC (digital down converter). We concentrate on the digital band-pass filters (BPFs) and Hilbert transform. The power amplifiers and the analog filters are not included at this point. The investigated waveforms are the LFM, Alltop and Björck waveforms [6].

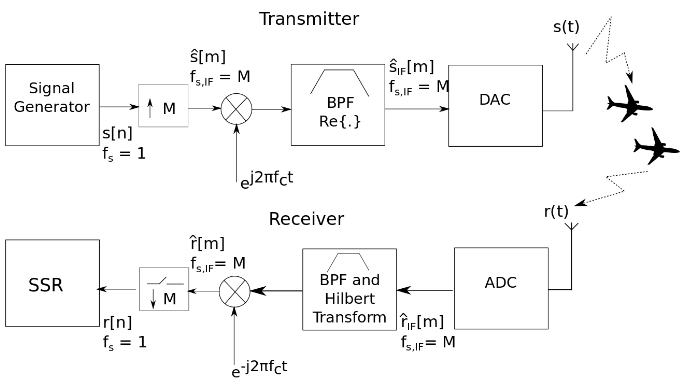

Fig. 1. Simplified block scheme of a generalized RF transmitter and receiver

After the initial sequences are generated at rate $f_s = 1$ they are interpolated to a new sequence $\hat{s}[m]$, at rate $f_{s,IF} = M$, in order to allow for digital up-conversion to intermediate frequency (IF). The initial LFM and Alltop sequence are linearly interpolated $\hat{s}[m] = (s[\lfloor m/M \rfloor + 1] - s[\lfloor m/M \rfloor])(m \operatorname{mod} M)/M + s[\lfloor m/M \rfloor]$, whereas the binary Björck is put on a rectangular pulse shape $\hat{s}[m] = s[\lfloor m/M \rfloor]$ in order to keep it binary , where $m = 0, 1, \ldots, ML - 1$, $n = 0, 1, \ldots, L - 1$ and $\lfloor \cdot \rfloor$ denotes the floor function. After the up-conversion the resultant signal is filtered to constrain its bandwidth and to filter any harmonics from the mixing.

The receiver basically does the inverse of the transmitter, starting with the ADC which samples $r(t)$ at rate $f_{s,IF} = M$. We use the Hilbert transform to recover the complex signal and another low-pass filter (LPF) which precedes the final down-sampling to the initial rate $f_s = 1$.

The double sided bandwidth B_{f} of all the filters is tunable and is relative to the reference sampling frequency $f_s = 1$.

3.1. Sparse signal recovery (SSR)

Several SSR methods [7] are available for implementation in CS radar. We prefer a Bayesian approach, implemented using the complex fast Laplace (CFL) algorithm because it is robust to noise and is executed in nearly real time (note that the FL from [8] is adapted to complex signals in [9]).

In traditional radar processing, the matched filter (MF):

$$\mathbf{x}_{\text{MF}} = \mathbf{S}^H \mathbf{y} \tag{3}$$

is the test statistics for a likelihood based detection and estimation. The Bayesian approach delivers an SSR estimator:

$$\mathbf{x}_{\text{SSR}} = \arg\min_{\mathbf{x}} \{ |\mathbf{y} - \mathbf{S}\mathbf{x}|^2 + \lambda ||\mathbf{x}||_1 \}, \tag{4}$$

where the parameter λ balances between the noise energy and the sparsity.

4. COHERENCE AND OPTIMIZATION

4.1. Optimization of the ACF

The coherence of the model matrix $\mathbf{S}$ in (2) depends on the shape and bandwidth of the transmitted pulse. Minimization of the coherence is equivalent to minimizing the power in the off-peak correlations of the ACF of the transmitted waveform [6], corresponding to the optimization problem $\min ||\mathbf{S}^H\mathbf{S} - \mathbf{I}||_F^2$. Because of the difficulty of solving this quadratic optimization problem, we minimize the average coherence of the waveforms [6]. We adopt the algorithm of [10] to solve the optimization problem and present the results in Fig. 2(note that for this optimization, we assume $Q = 1$ and $C = 1$).

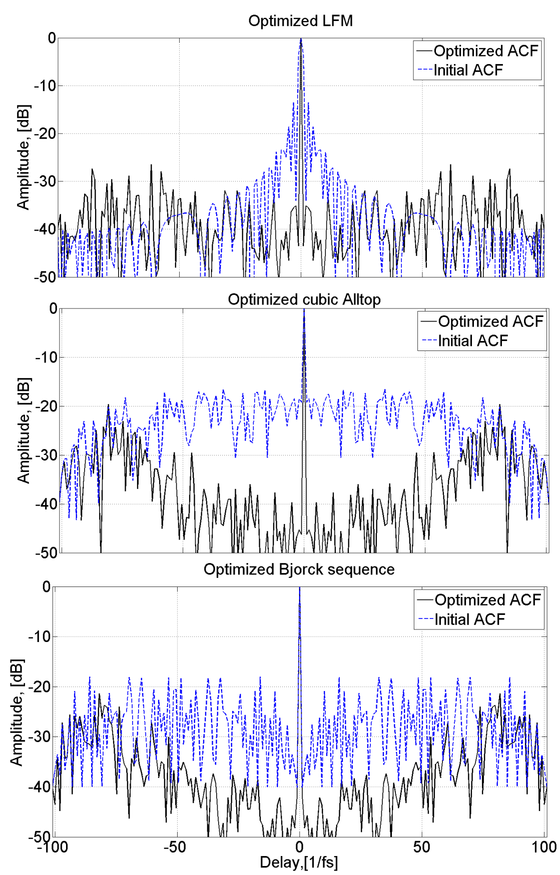

Fig. 2. Optimized waveforms

Optimization of the LFM decreases the width of the main lobe and removes the sinc structure of the ACF. For the optimized Alltop and Björck, the sharp response at zero delay remains and the off-peak correlations are reduced.

4.2. Coherence of an underdetermined system

Up-sampling of the estimation grid to a cell size of $\Delta\tau = 1/(Qf_s)$, with $Q > 1$ equates to finer sampling of the transmitted waveform in (2), which increases the correlation between the columns of $\mathbf{S}$, as shown in Table 1. Increasing Q, quite drastically reaches the maximum coherence $\mu(\mathbf{S}) \approx 1$.

On the other hand, compression by a partial Fourier matrix $\mathbf{\Phi}$ yields better coherence, even for $C = 4$, as shown in Table 2.

Table 1. Coherence of $\mathbf{S}$ with up-sampled estimation grid

Waveform	Q = 1	Q = 2	Q = 4	Q = 8
LFM	-3.9dB (0.64)	-0.91dB (0.9)	-0.22dB (0.97)	-0.05dB (0.99)
Alltop	-16.6dB (0.15)	-3.18dB (0.7)	-0.55dB (0.94)	-0.13dB (0.98)
Björck	-18dB (0.13)	-3.25dB (0.68)	-0.6dB (0.93)	-0.14dB (0.98)

Table 2. Mutual coherence $\mu(\mathbf{\Phi S})$, where $\mathbf{\Phi}$ is a partial Fourier matrix.

Waveform	C = 1	C = 2	C = 4	C = 8
LFM	-3.9dB (0.64)	-3.82dB (0.64)	-3.82dB (0.64)	-4.06dB (0.67)
Alltop	-16.6dB (0.15)	-12.53dB (0.23)	-9.61dB (0.33)	-6.83dB (0.45)
Björck	-18dB (0.13)	-14.3dB (0.19)	-12.17dB (0.25)	-8.25dB (0.38)

5. RESULTS

This section contains our results from SSR (4), as well as the MF-type of detection, where we assume an LFM sequence of length $L = 100$, and an Alltop and Björck sequence of length $L = 101$. The reconstruction results are averaged over 100 independent noise realizations, where we assume that SNR = 10 dB, which is defined as

$$\text{SNR} = \frac{\text{E}\{|s[n]|^2\}}{\text{E}\{|e[n]|^2\}} = \frac{1/L}{\sigma^2}, \tag{5}$$

where $\sigma^2 = B_f N_0$ is the bandwidth dependent noise variance. In our simulations, we fix the noise power spectral density N_0 and set $\sigma^2 = B_f N_0$, according to the B_f. In this way, we incorporate the effect of capturing more noise power by increasing B_f.

To evaluate the resolution capabilities of the waveforms, we take as spacing between two targets one reference resolution cell $1/f_s$ for $Q = 2$, half a reference cell $1/2f_s$ for $Q = 4$. In such a way, we can always see a possible false positive on a grid point between the two true targets.

The compression matrix $\mathbf{\Phi}$ contains P/C randomly selected rows from a $P \times P$ DFT matrix. In Fig. 7 and Fig. 8 we show the SSR and MF results, for $B_f = 1$ and $B_f = 2$.

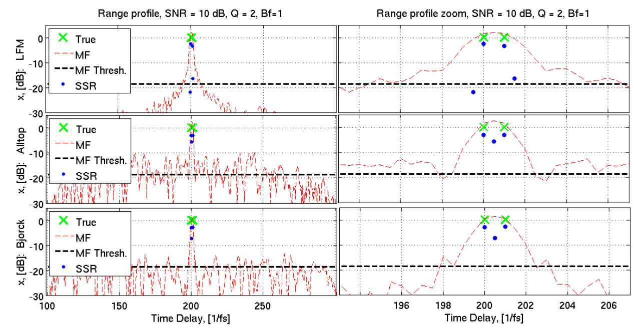

Fig. 3. MF and SSR with 2 targets SNR = 10 dB per target, $Q = 2$, $B_f = 1$.

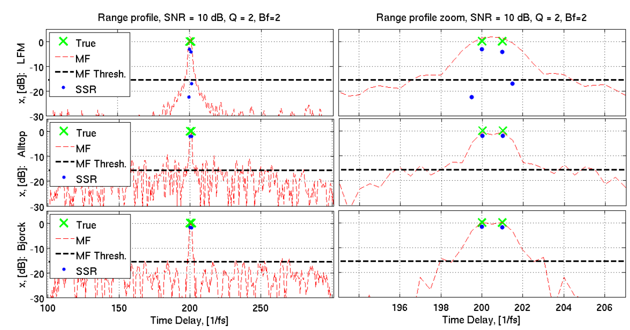

Fig. 4. MF and SSR with 2 targets SNR = 10 dB per target, $Q = 2$, $B_f = 2$.

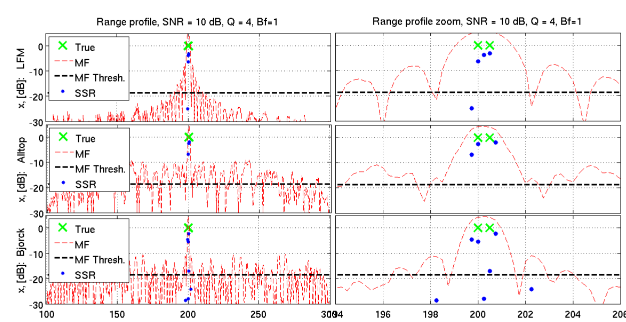

Fig. 5. MF and SSR with 2 targets SNR = 10 dB per target, $Q = 4$, $B_f = 1$.

Because of the good incoherence $\mu(\mathbf{S})$ in case $C = 4$, all three waveforms provide good reconstruction, if a wider filter

$B_f = 2$ is chosen. However, $B_f = 1$ results in false positives for Alltop and Björck.

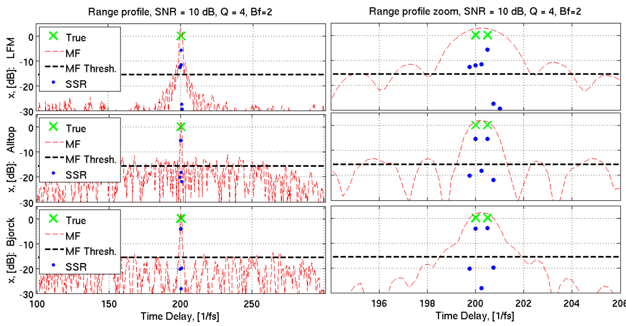

Fig. 6. MF and SSR with 2 targets SNR = 10 dB per target, $Q = 4$, $B_f = 2$.

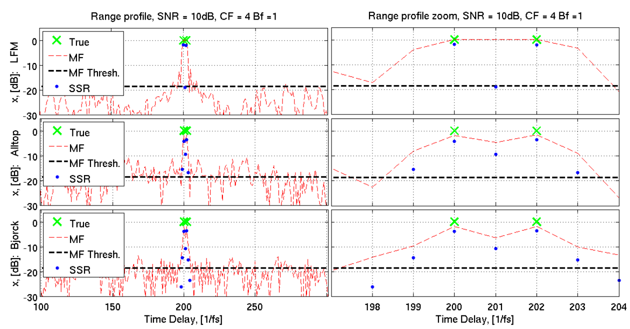

Fig. 7. MF and SSR with 2 targets SNR = 10 dB per target, $C = 4$, $B_f = 1$.

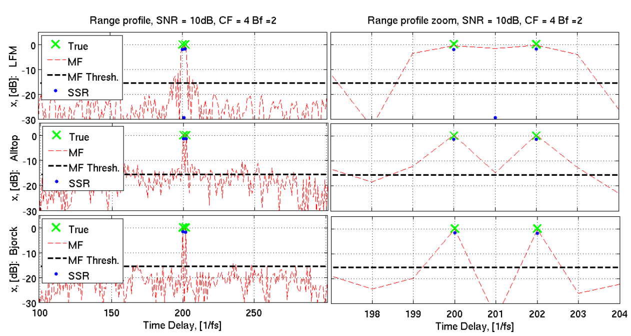

Fig. 8. MF and SSR with 2 targets SNR = 10 dB per target, $C = 4$, $B_f = 2$.

6. CONCLUSIONS

In this paper, we showed that in a digital CS-radar system, with a properly chosen B_f regarding the transmitted waveform, a higher range resolution than the conventional MF is achieved. Furthermore, a wider filter, capturing more noise, does not have a significant effect on the recovery process. However, increasing the resolution beyond $Q = 4$ yields a very coherent sensing matrix $\mathbf{S}$, resulting in false positives.

It was shown in [6] that B_f influences the sidelobes and the width of the main lobe in the ACF of the Alltop and Björck. Furthermore, by graphical comparison, the required B_f for Alltop is $B_f = 2$ and $B_f = 1$ for Björck sequences. However, here we showed that we actually need $B_f = 2$ for both sequences to perform optimally.

On the other hand, compressing the signal at the receiver, by applying a compression matrix $\mathbf{\Phi}$, keeps the uniqueness of the columns of $\mathbf{S}$. In that case $\mu(\mathbf{S})$ is not severely decreased, allowing good sparse reconstruction with all the investigated waveforms, for SNR = 10 dB. Also, the coherence of the initial waveforms can be reduced, while the behavior of those optimized waveforms in an actual system will be addressed in a following article.

7. REFERENCES

[1] M.A. Herman and T. Strohmer. High-resolution radar via compressed sensing. *IEEE Transactions on Signal Processing*, 57(6):2275 –2284, June 2009.

[2] Li K. Ling C. Gan, L. Novel toeplitz sensing matrices for compressive radar imaging. *COSERA*, May 2012.

[3] M.C. Shastry, R.M. Narayanan, and M. Rangaswamy. Compressive radar imaging using white stochastic waveforms. In *WDD, 2010 International*, 2010.

[4] G. Lellouch, R. Pribic, and P. Van Genderen. Merging frequency agile ofdm waveforms and compressive sensing into a novel radar concept. In *Radar Conference, 2009. EuRAD 2009. European*, pages 137–140, 2009.

[5] E.J. Candes and M.B. Wakin. An introduction to compressive sampling. *Signal Processing Magazine, IEEE*, 25(2):21–30, 2008.

[6] Pribić R. Zegov, L. and G. Leus. Optimal waveforms for compressive-sensing radar. *EUSIPCO*, September 2013, to appear.

[7] J.A. Tropp and S.J. Wright. Computational methods for sparse solution of linear inverse problems. *Proceedings of the IEEE*, 98(6):948 –958, june 2010.

[8] S.D. Babacan, R. Molina, and A.K. Katsaggelos. Bayesian compressive sensing using laplace priors. *Image Processing, IEEE Transactions on*, 19(1):53–63, Jan. 2010.

[9] R. Pribic and H. Flisijn. Back to Bayes-ics in radar: Advantages for sparse-signal recovery. *COSERA*, May 2012.

[10] P. Stoica, Hao He, and Jian Li. New algorithms for designing unimodular sequences with good correlation properties. *IEEE Transactions on Signal Processing*, 57(4):1415 –1425, April 2009.